Open Access Journal

Journal of Power Technologies 93 (4) (2013) 207–215

journal homepage:papers.itc.pw.edu.pl

Determination of Optimum Hysteresis Bandwidth to Improve the Operation of Electric Machines

Mohammad Ali Shamsi-Nejad[a], Mohammad Reza Khalghani[a], Mohammad Hassan Khooban[*,b]

[a] *Power Electronic and Drive Laboratory (PE&D)*
University of Birjand, Birjand, Iran
[b] *Department of Electrical and Electronic Engineering*
Shiraz University of Technology, Shiraz, Iran

Abstract

Many techniques have been presented for optimizing energy consumption in drive systems to increase efficiency. This paper presents a new method to reduce energy consumption in motor and drive systems. We can achieve an optimal point in term of current THD and switching loss with appropriate determining hysteresis bandwidth. To date, no study has been done in this field. Proposed in this paper are: (i) a proper bandwidth, and (ii) a new index to determine the aforementioned objectives in order to derive an appropriate hysteresis bandwidth.

Keywords: Energy optimization, Fuzzy membership function index, Hysteresis bandwidth, Motor current THD, Commutation loss

1. Introduction

Induction motors are currently in common use in various industries. Researchers have investigated various control methods to drive these motors. In light of the large overall consumption of energy by motors drives, enormous efforts have been made to optimize energy usage. Decreasing switching loss leads to reductions in energy consumption by drive systems, and decreasing current THD can bring about reductions in energy consumption by motors. Each proposed method is for a special purpose. These research topics include various inverter topologies, modulation methods, control and estimation approaches. Also, much researches have been done in the field of drive control techniques, including control by a variable voltage source with fixed frequency, v/f control, rotor resistance control, injecting voltage into a rotor circuit, direct torque control (DTC) and vector control. Of the foregoing, the best method is vector control, and it is this method that has been used in this paper.

Current and voltage source inverters are widely used in industries to supply induction motor drives. The widespread development of these inverters in industry led to much important researches being carried out in the field of modulation. Since the control methods of these inverters have a direct relationship with drive efficiency, further researches into improving them could boost efficiency and cut energy consumption. The main objective of any modulation technique is to obtain the best current and voltage waveforms with minimum commutation losses. The secondary objectives include: reducing common mode voltage, DC voltage balancing, reducing input

[*]Corresponding author
Email address: khooban@sutech.ac.ir (Mohammad Hassan Khooban[*])

current harmonics and reducing dv/dt.

While any of these objectives can be satisfied with an appropriate modulation method, it is nevertheless impossible to satisfy all of these objectives at the same time. Modulation techniques are classified into four main categories: Pulse Width Modulation (PWM), space vector modulation (SVM), harmonic control modulation and other variable commutation frequency methods (including hysteresis method) [1]. These modulation techniques for power inverters have been used for decades and many of them have evolved for commercial production.

In order to reduce motor voltage and current THD, the inverter must have a high commutation frequency. Thus the commutation loss increases and induces some currents in the shaft and bearings and also brings about some electromagnetic effects [2–4]. Torque ripple causes speed fluctuations, mechanical vibrations and sonic noises [5]. Current harmonics cause overheating of windings which cause serious problems in motors. This effect is seen especially in large motors in which their skin effect is more important [4].

Motor efficiency is directly proportional to the quality of input current. Therefore, motor efficiency decreases as the current waveform harmonics increase. If hysteresis bandwidth reduces, the harmonics reduce too.

Other generalized PWM approaches include subharmonics or sinusoidal pulse width modulation (SPWM), selective harmonic eliminated pulse width modulation (SHEPWM), space vector modulation (SVM) etc. [6–9]. These methods have some disadvantages such as: high commutation frequency, high dv/dt, generation of common mode voltage, need for a transformer in high voltage motors, some harmonic components and low power delivery capacity [10].

Passive LC filters and/or APF[1]s are used to decrease harmonic waveforms. Passive filters have some disadvantages, such as: large size, resonance problems and fixed compensation characteristics [11]. It is more efficient to use an APF system. The main advantages of using an APF are: elimination of unwanted harmonics, power factor correction, redistribution of power to keep the system in balanced position, EMI reduction [12]. In [13], a filter was proposed with a nonlinear control method that has shown the desired performance on motor parameters but this solution is complicated.

The existence of these problems in certain presented methods led the authors of this paper to introduce a novel method. This method was used to maintain motor power quality parameters and reduce inverter commutation loss without any complexity in the control system. In this paper, it will be shown that by choosing an appropriate hysteresis bandwidth, we can have optimum current THD and inverter commutation loss for a motor.

As was mentioned earlier, commutation frequency increases with small hysteresis bandwidth and vice versa. If the commutation frequency increases, the current THD of motor decreases, but some problems such as greater commutation loss occur. Therefore, a compromise should be reached between commutation frequency and current quality [14]. In this paper, by selecting an appropriate hysteresis bandwidth, optimization is attempted of an objective function with two objectives: THD of electrical current of motor and inverter commutation loss. Also, the fuzzy membership function method is used to make the dimensions of objective functions uniform. Furthermore, the proposed method can create an index to give priority to the aforementioned objectives depending on the ideas of the designer.

Section 2 of this paper puts forward the dominant relationships on inverter commutation loss. Section 3 deals with the results of THD variation rate of motor current and commutation loss due to increasing the hysteresis band width. Section 4 explains in detail the proposed method and simulation approach.

2. Vector control method

The vector control method was introduced for the first time about three decades ago. The basic idea was based on decoupling motor parameters in quadrature q and direct d fields [15] (Park's transformation). This was instead of the coherency of parameters on the condition of rotor and the coupling between phases of rotor and stator that have time transitive coefficients; time transitive parameters are also omitted. The vector control method di-

[1] Active Power Filter

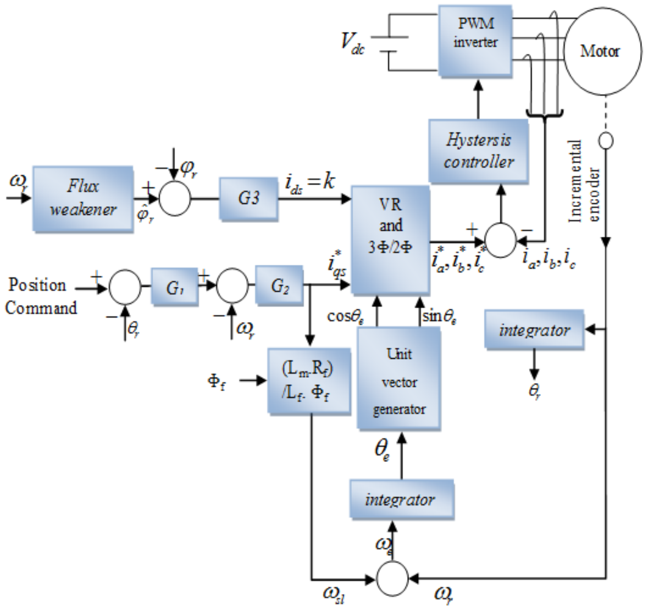

Figure 1: Indirect vector control diagram block

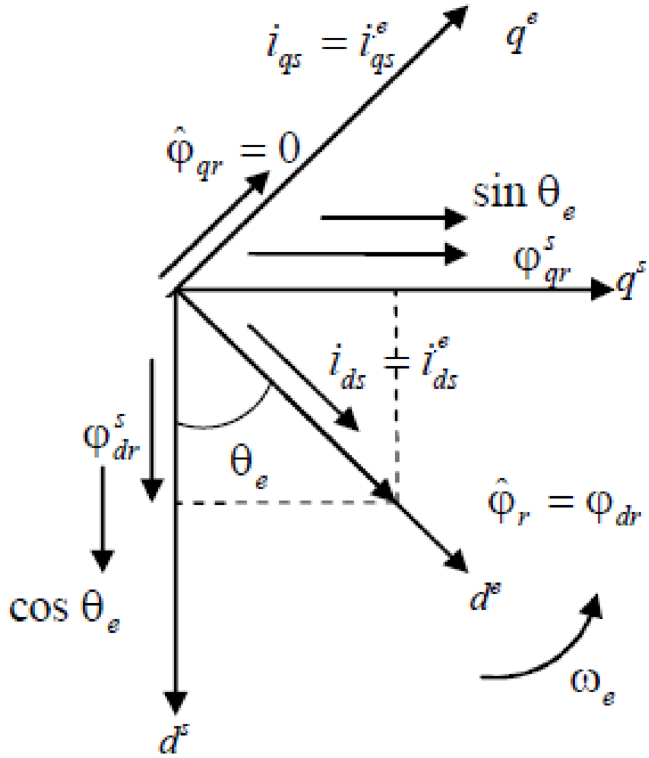

Figure 2: Indirect vector control phasor diagram

vides into two direct and indirect methods, with the difference between them being in the way unit vectors are produced. In the direct method unit vectors are calculated using flux signals whereas in the indirect method speed signals ω_r and slip frequency ω_{sl} are used Due to the poor operation of flux sensors at low speeds and position control, the more common way is the indirect method [16], which is also used in this paper. The indirect vector control block diagram is shown in Figure 1.

According to Figure 2 d^s–q^s are the stationary reference frame. Also the direct and quadrature axes (d^e–q^e) are synchronously rotating the reference frame direct and quadrature axes. Angel θ_e is expressed with the sum of rotor angel θ_r and slip angle θ_{sl}.

Flux equations in the equivalent circuit of d^e–q^e frame for the induction motor are expressed in (1), (2).

$$0 = \frac{R_r}{L_r}\psi_{rd} + \frac{d}{dt}\psi_{rd} - \frac{L_o}{L_r}R_r i_{sd} - \omega_{sl}\psi_{rq} \tag{1}$$

$$0 = \frac{R_r}{L_r}\psi_{rq} + \frac{d}{dt}\psi_{rq} - \frac{L_o}{L_r}R_r i_{sq} - \omega_{sl}\psi_{rd} \tag{2}$$

Rotor flux is placed in direct axis d^e, therefore:

$$\psi^e_{dr} = \psi_r \tag{3}$$

$$\frac{d\psi^e_{dr}}{dt} = 0 \tag{4}$$

$$\psi^e_{qr} = \frac{d\psi^e_{qr}}{dt} \tag{5}$$

We can estimate direct axis current and slip frequency versus stator reference current i^e_{qs} and motor parameters by replacing Equations (3) ~ (5) in (1) and (2):

$$i^e_{ds} = \frac{\psi_r}{L_m} \tag{6}$$

$$\omega_{sl} = \frac{L_m}{\psi_r}\frac{R_r}{L_r}i^e_{qs} \tag{7}$$

According to Figure 1, the induction motor is energized by the current controlled PWM inverter which operates as a sinusoidal three-phase current source. Motor speed ω_r is compared to reference speed ω^*_r and the resulting error will be processed by the speed controller to produce stator's quadrature axis current

i^*_{qs}. Motor torque and flux are controlled independently by the stator's quadrature axis current and the stator's direct axis current respectively [16]. Therefore flux magnitude in vector control in q^e direction is zero and quadrature axis current is given by (1):

$$i^e_{qs} = \frac{2}{3}\frac{2}{p}\frac{L_r}{L_m}\frac{T_e}{\psi_{dr}} \tag{8}$$

The angle of synchronously rotating frame θ_e depends on rotor speed ω_m and slip frequency as in the following equation:

$$\theta_e = \int (\omega_m + \omega_{sl})\, dt \tag{9}$$

Reference currents i^e_{qs} and i^e_{ds} are converted to phase reference currents i^e_a, i^e_b and i^e_c for the current regulator.

The hysteresis controller determines inverter gate signals by comparing real and reference three phase currents. Every error signal resulting from these currents passes a bandwidth. Then they frequently arrive at the borders and inverter gate signals are produced at these times. The controller performs this task by determining the appropriate hysteresis bandwidth. This paper is concerned with determining an appropriate value for it.

3. Calculating commutation losses in the voltage source inverter (VSI)

Switching losses are divided into two types: commutation and conduction losses. We are going to progress a way for evaluations of commutation losses in the following.

These losses occur just at the time of switching. If a switch is turned on (or off), the switch voltage reduces (increases) and the switch current increases (reduces). During the switching, the commutation loss is gained from the multiplication of current and voltage. Some methods are introduced in order to calculate these losses in each period [7].Two schemes for computing commutation losses are set out below.

3.1. First method

This way is based on evaluating the switching times of each switch. First, it is essential to identify the commutation times of switches, then at these times determine the values of voltage and current and evaluate the energy wasted during each commutation using the components characteristics obtained from the company. We assume that "ε" is the time of commutation. Using the abacuses obtained from the company, the wasted energy during the turn on or turn off period of each switching is a function of switch voltage and current. Of note, the loss energy of diodes within the turn on period is insignificant.

If a switch is turned on, the anti-parallel diode of complementary switch (in this same leg) is turned off. These two components drive alike voltage and current. For example, in phase "a", at the time the top switch (Th) is turned on, the wasted energy is gained in the switch and bottom diode (Db) by:

$$\begin{aligned} E_a(t_0) &= E_{com\,on,Tha}(t_0) + E_{com\,off,Dba}(t_0) \\ &= \tfrac{1}{\varepsilon}\int_{t_0}^{t_0+\varepsilon} [K_1 + K_2 \cdot i_{Tha}(t)] \cdot v_c(t) \cdot sg(i_a) \cdot dt \end{aligned} \tag{10}$$

Where K_1 and K_2 are given by the abacus. E_{comon}, E_{comoff} are wasted commutation energy at the time of turn on and turn off in each diode or IGBT respectively. The forward voltage drop of the switch is shown as "v_c". The existence of the signs function $[sg(i_a)]$ prevents consideration of the non-existent losses while the phase current is not positive. In this case, the phase current changes from the bottom diode towards the top switch. The evaluation of the commutation losses (P$_{conm}$) in phase "a" (this first inverter leg) in the time period $[t_1, t_2]$ is equal to:

$$\begin{gathered} P_{com.on\,Tha} + P_{com.Dba} = \tfrac{1}{T}\int_{t_1}^{t_2}[K_1 + K_2 i_{Tha}(t)] \cdot v_c(t) \cdot sg(i_a) \cdot C_{ha} dt \\ P_{com.off\,Tba} = \tfrac{1}{T}\int_{t_1}^{t_2}[K_3 + K_4 i_{Tba}(t)] \cdot v_c(t) \cdot \overline{sg(i_a)} \cdot \bar{C}_{ba} dt \\ P_{com.off\,Tha} = \tfrac{1}{T}\int_{t_1}^{t_2}[K_3 + K_4 i_{Tha}(t)] \cdot v_c(t) \cdot sg(i_a) \cdot \bar{C}_{ha} dt \\ P_{com.on\,Tba} + P_{com.Dha} = \tfrac{1}{T}\int_{t_1}^{t_2}[K_1 + K_2 i_{Tba}(t)] \cdot v_c(t) \cdot \overline{sg(i_a)} \cdot C_{ba} dt \end{gathered} \tag{11}$$

Then the overall commutation loss in one inverter leg (for example, phase "a") is obtained by:

$$\begin{gathered} P_{total\,com.} = (P_{com.on\,Tha} + P_{com.\,Dba}) + P_{com.off\,Tba} \\ +(P_{com.Dha} + P_{com.on\,Tba}) + P_{com.off\,Tha} \end{gathered} \tag{12}$$

Also the overall three phase loss (commutation and conduction) of the voltage source inverter (VSI) is:

$$P_{total} = 3\,(P_{total\,com.} + P_{total\,cond.}) \tag{13}$$

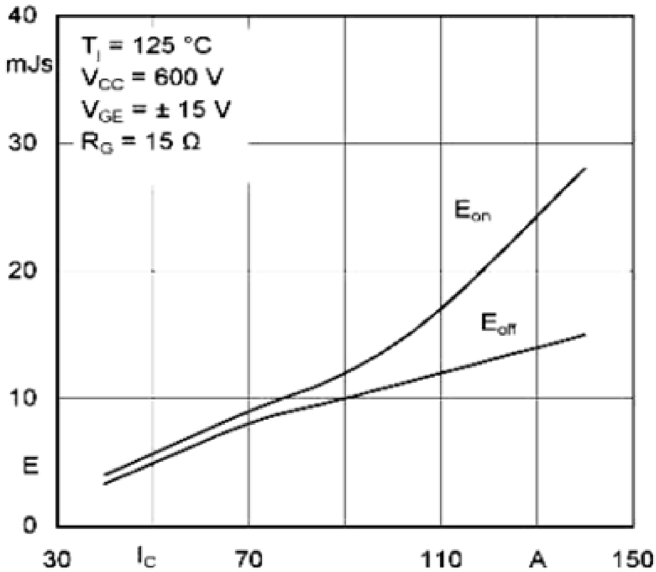

Figure 3: Wasted energy in conduction/blockage (E_{on}/E_{off}) as a function of collector current (I_C) [7]

The commutation time "ε" is not recognized and the coefficients K_1, K_2, K_3 and K_4 are unknown. Therefore, use of the first method is not always practical. Another scheme is suggested [7].

3.2. Second method

This scheme is based on direct computation of commutation loss and uses the component characteristics given by the companies. This scheme to compute commutation losses requires the current value during every commutation period. Figure 3 reveals the overall loss of diode and switch during the conduction period and blocking period for an IGBT SKM 100GB123D.

The curves demonstrate the energy wasted from the IGBT switch and the diode:

$$\begin{cases} E_{on} = E_{com.on\,T} + E_{com.off\,D} \\ E_{off} = E_{com.off\,T} + E_{com.on\,D} \end{cases} \tag{14}$$

This way we do not require the commutation time. Using power supply voltage (V_{cc}), gate-emitter voltage (V_{GE}), junction temperature (T_j), collector current (I_C) and gate resistance (R_G) we can achieve directly at commutation losses [7].

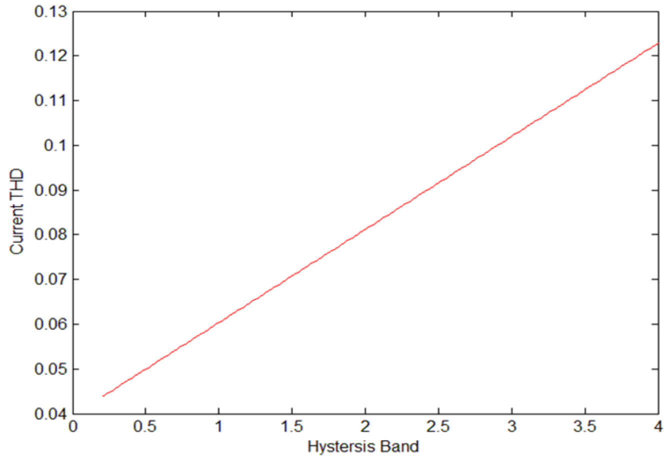

Figure 4: Current THD variations versus hysteresis bandwidth

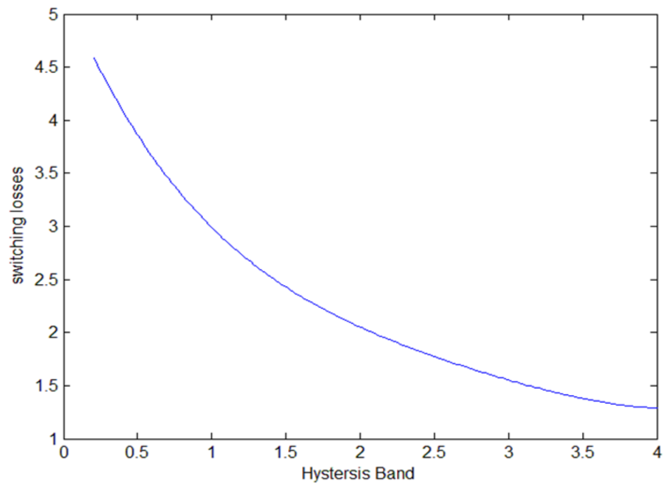

Figure 5: Commutation loss variation versus hysteresis bandwidth

4. Effect of hysteresis bandwidth on the motor current THD and commutation loss

This section simulations show the effect of hysteresis bandwidth on the motor current THD and commutation loss. In order to do this, a motor with specific parameters is simulated in torque control mode. Figure 4 shows the motor current THD variations due to increase in hysteresis bandwidth. Figure 5 shows variations of commutation loss values due to hysteresis bandwidth.

The variations of THD and commutation loss are plotted in [0.2 4] intervals of hysteresis bandwidth. These two figures can prove the mentioned claim in section 1. It is clear that increasing the hysteresis bandwidth leads to reductions in commutation loss and increases in current THD. These variation rates are not similar. According to Figures 4 and 5, current THD curve can be expressed as a linear algebraic equation, but commutation loss variation can be considered as an exponential rate. It should be noted that the small disturbances in these figures have been eliminated by filtering.

5. Fuzzy membership functions for current THD and commutation loss objectives

Fuzzy sets are used to have more control over the priorities of these two objectives (current THD and commutation loss). In other words, first both objective functions are placed in a membership function [17–20], then their linear combination is considered as the fuzzy desirability. As was mentioned before, fuzzy membership functions are combined by considering importance factors which depend on the designer's ideas [21]. Consequently, fuzzy membership functions are obtained as follows:

$$Maximize \quad F = w_1 \cdot \mu_T + w_2 \cdot \mu_L \qquad (15)$$

According to equation (6), increasing the fuzzy desirability function increases system desirability. In this equation w_1 and w_2 are the importance factors for each objective, whereas μ_T and μ_L are membership functions for the THD and commutation loss objectives respectively.

Now, we can introduce the membership functions for each objective. These objective functions can be created by determining appropriate weight coefficients according to each of the objectives and the designer's idea. Considering their importance and their effect on the system, weight coefficients are selected in such a way that their sum becomes equal to unity. Membership functions for optimization objectives which express the variations of the related objective in [0, 1] interval, may take various forms based on the type of problem [21].

To fuzzify the motor input current, its value is placed in the following membership function:

$$\mu_T = \begin{cases} \frac{T_{max}-T}{T_{max}-T_{min}} & for \quad T_{min} \le T \le T_{max} \\ 1 & for \quad T \le T_{min} \\ 0 & for \quad T \ge T_{max} \end{cases} \qquad (16)$$

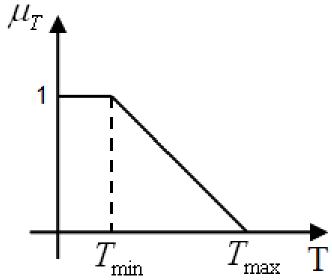

Figure 6: Membership function of motor input current

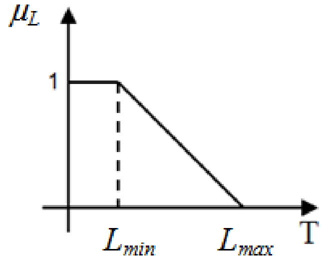

Figure 7: Memberships function for commutation loss

In this paper, T_{max} and T_{min} are considered as the maximum and minimum values of obtained THD. T is input current THD. This membership function is shown in Figure 6.

To fuzzify inverter commutation loss, its value is placed in the membership function of Equation (8).

$$\mu_L = \begin{cases} \frac{L_{max}-L}{L_{max}-L_{min}} & for \quad L_{min} \le L \le L_{max} \\ 1 & for \quad L \le L_{min} \\ 0 & for \quad L \ge L_{max} \end{cases} \qquad (17)$$

In this paper, L_{min} and L_{max} are considered as the maximum and minimum values of the obtained commutation loss and L is commutation loss. This membership function is shown in Figure 7.

6. Simulation and Results

To simulate the proposed idea, we use the indirect vector control method to drive the induction motor. The indirect vector control method is presented in Figure 1. Firstly, the objectives "current THD" and "commutation loss" are considered as two main objectives for determining hysteresis bandwidth. These parameters are in Per-Unit. In order to do this, variation curves of these two parameters due to the change

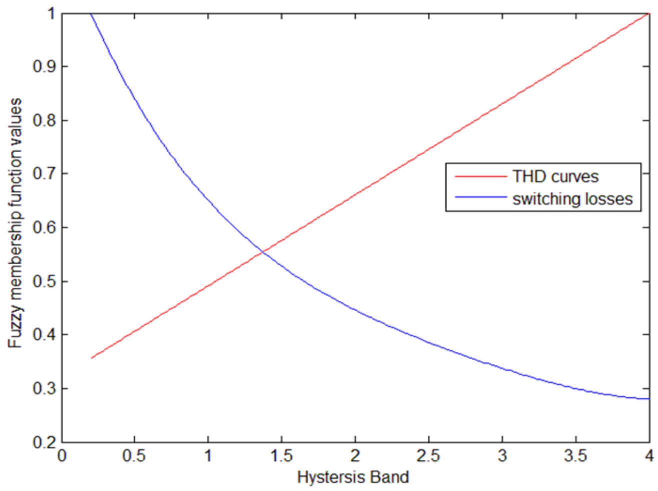

Figure 8: Per-Unit diagram for current THD and commutation loss versus hysteresis bandwidth

Table 1: The results obtained from current THD and commutation loss indices for different bandwidths

Hysteresis bandwidth	current THD	commutation loss	Fuzzy desirability function value
$B_h = 4$	0.1228	1.2886	0.5
$B_h = 2$	0.0813	2.0479	0.6479
$B_{hoptimum} = 1.378$	0.0682	2.5439	0.6555
$B_h = 0.5$	0.05	3.8532	0.5728
$B_h = 0.25$	0.0449	4.4451	0.5159

in hysteresis bandwidth are obtained. The intersect point of these two curves can be the best point for both current THD and commutation loss indices. Figure 8 shows these curves.

In order to verify this claim, the values of these indices in different hysteresis bandwidths and also in optimum bandwidth are shown in Table 1.

As can be seen, the best bandwidth for both objects is introduced. This result can be observed by comparing the obtained values for both indices in other bandwidths. The fuzzy desirability function value is also determined in Table 1. These values can be used to show the validity of the proposed method. According to this table, $B_{hoptimal} = 1.378$ is the optimum point for hysteresis bandwidth to improve current THD and commutation loss. It is the intersection point of the THD and commutation loss curves and has the highest fuzzy desirability.

Table 2: Optimal hysteresis bandwidth for different importance factor in fuzzy desirability function

Different importance factor	The best bandwidth
$w_1 = 0.5, w_2 = 0.5$	1.549
$w_1 = 0.4, w_2 = 0.6$	2.138
$w_1 = 0.7, w_2 = 0.3$	0.561

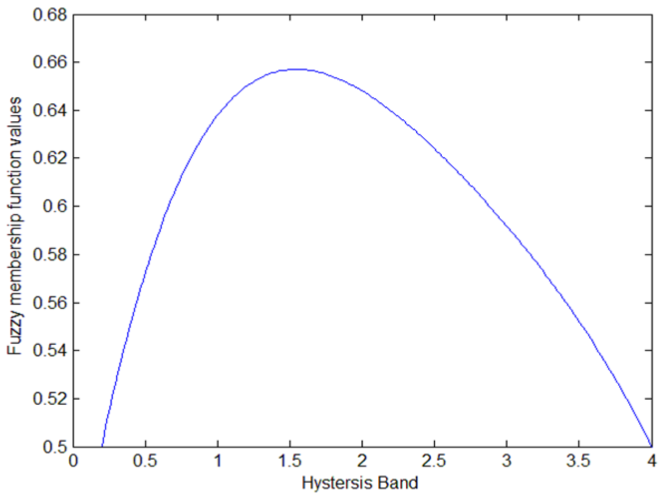

Figure 9: Fuzzy membership function value versus hysteresis band width for importance factors of $w_1 = 0.5$ and $w_2 = 0.5$

If the designer wants to have a specific priority on these two objectives, fuzzification of objectives can be used in the way that was explained in section 4. Now, results for 3 types of prioritizing on objects are given in Table 2. Clearly, the most desirable bandwidth in each case is correspondent with the maximum value of the fuzzy objective function in that case.

Fuzzy desirability curves versus hysteresis bandwidth for three states are shown in Table 2 and Figures 9, 10 and 11.
According to Table 1, the obtained results from Table 2 and Figures 8, 9 and 10, if the hysteresis bandwidth is determined with regard to a specific purpose, it can have more desirable effects on THD and inverter commutation loss.

The motor parameters used in the simulation are given in Table 3.

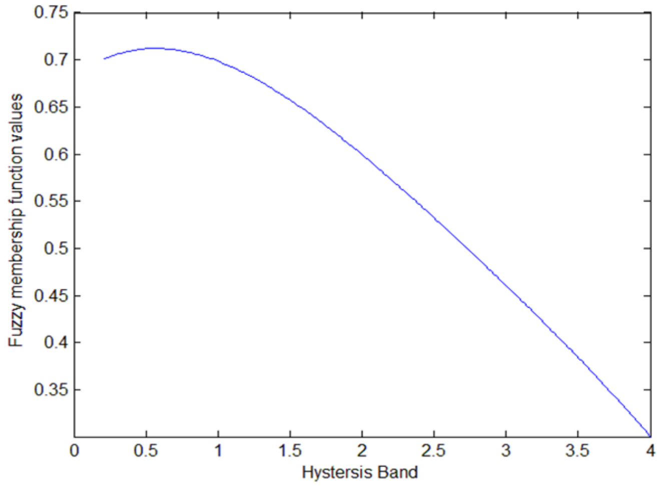

Figure 10: Fuzzy membership function value versus hysteresis band width for importance factors of $w_1 = 0.7$ and $w_2 = 0.3$

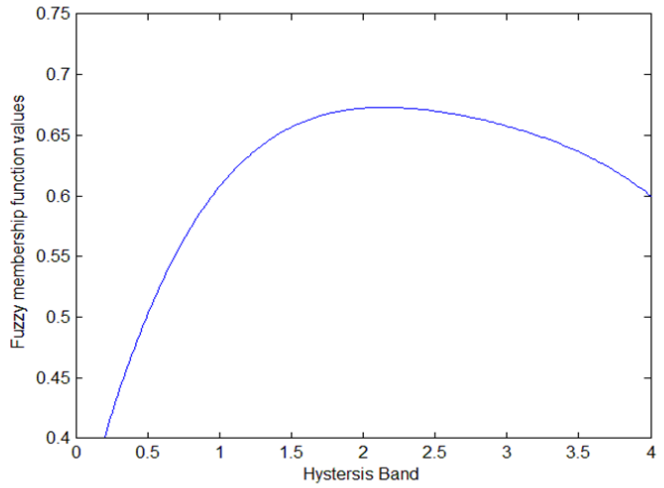

Figure 11: Fuzzy membership function value versus hysteresis band width for importance factors of $w_1 = 0.4$ and $w_2 = 0.6$

7. Conclusions

In this paper we reported variation rates of current THD and switching loss versus hysteresis bandwidth. The current THD has linear variation and the variation rate of switching loss is about exponential. As can be seen from the results of the proposed algorithm, input current THD can be improved significantly by an appropriate determination of the hysteresis band. By adopting the proposed algorithm, current THD and switching loss can be improved without using a special structure in drive and without using complex controllers. Also, a proper index is presented for giving preference to each objective cited. Consequently, optimization is achievable in economic terms and with respect to system maintenance.

Table 3: Parameters of simulated motor

Motor's parameters			
P_n	Rated power	60	(hp)
Vin	Rated voltage	460	(V)
R_s	Stator resistance	0.09961	(Ω)
L_s	Stator inductance	0.867	(mH)
$R_{r'}$	Rotor resistance	0.05837	(Ω)
L_m	Core inductance	30.39	(mH)
J	Motor inertia	0.04	(kg·m^2)

References

[1] M. P. Kazmierkowski, L. G. Franquelo, J. Rodriguez, M. A. Perez, J. I. Leon, High-performance motor drives, IEEE Industrial Electronics Magazine.

[2] R. J. Kerkman, Twenty years of pwm ac drives: When secondary issues become primary concerns, in: Proc. IECON'96, Taipei, Taiwan, R.O.C., 1996, pp. lvii–lxiii.

[3] A. M. Trzynadlowski, N. Patriciu, F. Blaabjerg, J. K. Pedersen, A hybrid, current-source/voltage source power inverter circuit, IEEE Trans. Power Electron. 16 (6) (2001) 866–871.

[4] M. Imecs, A. M. Trzynadlowski, I. I. Incze, C. Szabo, Vector control schemes for tandem converter fed induction motor drives, IEEE Trans. Power Electronic 20 (2) (2005) 493–501.

[5] J. Rodriguez, J.-S. Lai, F. Z. Peng, Multilevel inverters: A survey of topologies, controls, and applications, IEEE Trans. On Industrials Electronics 49 (4).

[6] K. Gulez, A. A. Adam, H. Pastaci, Improving the performance of hysteresis direct torque control of ipmsm using active filter topology, Sadhana 32 (2006) 245–258.

[7] M. A. Shamsi-Nejad, S. Pierfederici, F. Meibody-Tabar, A new pwm regulator to minimize the inverter losses, in: IEEE Conference on Computer Applications and Industrial Electronics, Penang, Malaysia, 2011, pp. 82–86.

[8] K. Marouani, M. Khaldi, F. Khoucha, A. Kheloui, Switching losses and harmonic currents evaluation of pwm techniques forvsi-fed dual stator induction motor drive, in: IEEE Conference, 17th Mediterranean Conference on Control& Automation, Thessaloniki, Greece, 2009.

[9] N. R. S. Reddy, T. B. Reddy, J. Amarnath, D. S. Rayudu, Space vector based minimum switching loss pwm algorithms for vector controlled induction motor drives, in: IEEE Conference, India, 2010.

[10] L. M. Tolbert, F. Z. Peng, Multilevel converters for large electric drives, in: IEEE/APEC, Anaheim, CA, USA, 1998, pp. 530–536.

[11] B. L. Cortes, M. S. Horta, S. A. Claduio, G. V. M. Cardenas, Single-phase active power filter for reactive power and harmonic compensation, in: Power Electronics Congress, 1998. CIEP 98. VI IEEE International, 1998, pp. 184–187.

[12] K. Gulez, I. Aliskan, T. V. Mumcu, G. Cansever, Neural network based control of ac-ac converter for voltage sags, harmonics and emi reduction, Lecture Notes in Computer Science 4681 (2007) 534–544.

[13] Y. A. I. Aliskan, K. Gulez, Spoiler effects reduction with using active power filter on a direct torque controlled induction machine, Turk J Elec. Eng. & Comp Science 19 (5).

[14] M. P. Kazmierkowski, R. Krishnan, F. Blaabjerg, Control in power electronics: Selected Problems, Academic Press, 2002.

[15] O. S. Ebrahim, M. F. Salem, P. K. Jain, M. A. Badr, Application of linear quadratic regulator theory to the stator field-oriented control of induction motors, IET Electric Power Applications (2009) 637–646.

[16] M. R. Khalghani, M. A. Shamsi-Nejad, K. Beyki, An intelligent controller for optimal vector control of induction motor, in: Computer Applications and Industrial Electronics, Malaysia, Penang, 2011, pp. 78–81.

[17] M. H. Khooban, A. Alfi, D. Nazari Maryam Abadi, Control of a class of nonlinear uncertain chaotic systems via an optimal type-2 fuzzy pid controller, IET Science, Measurement and Technology 7 (2013) 50–58. doi:10.1049/iet-smt.2012.0092.

[18] M. H. Khooban, M. R. Soltanpour, D. Nazari, Z. Esfahani, Optimal intelligent control for hvac systems, Journal of Power Technologies 92 (3) (2012) 192–200.

[19] M. H. Khooban, M. R. Soltanpour, Swarm optimization tuned fuzzy sliding mode control design for a class of nonlinear systems in presence of uncertainties, Journal of Intelligent and Fuzzy Systems 24 (2) (2013) 383–394. doi:10.3233/IFS-2012-0569.

[20] M. H. Khooban, A. Alfi, D. Nazari Maryam Abadi, Teaching-learning-based optimal interval type-2 fuzzy pid controller design: A nonholonomic wheeled mobile robots, Robotica 31 (7) (2013) 1059–1071. doi:10.1017/S0263574713000283.

[21] M. R. Khalghani, M. A. Shamsi-Nejad, M. Farshad, M. H. Khooban, Modifying power quality indices of load by presenting an adaptive method based on hebb learning algorithm for controlling dvr, Automatika – Journal for Control, Measurement, Electronics, Computing and CommunicationsIN PRESS.